Free Radical Research, April 2010; 44(4): 410–421

informa
healthcare

Proteomic characterization of the striatum and midbrain treated with 6-hydroxydopamine: Alteration of 58-kDa glucose-regulated protein and C/EBP homologous protein

YOKO OGAWA AKAZAWA[1], YOSHIRO SAITO[1,2], KEIKO NISHIO[1], MASANORI HORIE[1], TOMOYA KINUMI[1], YOSHINORI MASUO[3], YASUKAZU YOSHIDA[1], HITOSHI ASHIDA[4] & ETSUO NIKI[1]

[1] Health Technology Research Center, National Institute of Advanced Industrial Science and Technology (AIST), Kansai Center, Ikeda, Osaka, Japan, [2] Department of Medical Life Systems, Faculty of Medical and Life Sciences, Doshisha University, Kyotanabe, Kyoto, Japan, [3] Health Technology Research Center, AIST, Tsukuba West, Tsukuba, Japan, and [4] Department of Agrobioscience, Graduate School of Agricultural Science, Kobe University, Kobe, Hyogo, Japan

(Received date: 15 September 2009; In revised form date: 27 November 2009)

Abstract

The present study performed proteomic analysis of the midbrain and striatum of 6-hydroxydopamine (6-OHDA)-treated neonatal rats—a model of attention-deficit hyperactivity disorder (ADHD). Proteomic analysis revealed that a 58-kDa glucose-regulated protein (Grp58) was temporarily phosphorylated and its level was elevated by 6-OHDA. Furthermore, 6-OHDA increased the expression level of C/EBP homologous protein (CHOP), a mediator of endoplasmic reticulum (ER) stress response, in the midbrain and striatum. *In vitro* experiments using PC12 cells revealed that 6-OHDA or hydrogen peroxide could induce the elevation of Grp58 and CHOP. 6-OHDA could induce the elevation of Grp58 and CHOP in the presence of catalase, a hydrogen peroxide-removing enzyme, suggesting that the elevation of Grp58 and CHOP are induced by both hydrogen peroxide and *p*-quinone generated by 6-OHDA. Collectively, these findings suggest that ER stress involving the alteration of Grp58 and CHOP play a significant role in the induction of insults by 6-OHDA *in vivo*.

Keywords: *6-Hydroxydopamine, hydrogen peroxide, p-quinone, Grp58, CHOP.*

Introduction

6-Hydroxydopamine (6-OHDA) is a selective catecholaminergic neurotoxin that has been widely used to generate Parkinson's disease (PD) models *in vitro* and *in vivo*; it is known to induce toxicity that mimics the neuropathological and biochemical characteristics of PD [1]. It has also been reported that neonate rats with 6-OHDA-induced lesions on post-natal day 5 exhibit behavioural hyperactivity similar to that observed in attention-deficit hyperactivity disorder (ADHD) [2]. PD and ADHD models are induced by the depletion of dopamine in the striatum, which leads to a wide variety of behavioural changes such as motor dysfunction and hyperactivity [1,3]. In this ADHD model, we have previously reported that spontaneous motor activity is significantly increased in 4–5-week-old 6-OHDA-treated neonatal rats [2–4]. Alterations have been observed in several classes of gene expression, depending on the brain region; for example, enhanced expression of the glutamate transporter gene in the striatum and increase of the expression of the dopamine receptor D4 and dopamine transporter in the midbrain, mimicking human hyperkinesias in both behaviour and gene expression [2,4]. Dopamine content, but not noradrenaline content, was reported to dramatically decrease in the striatum of ADHD rats [3,4]; however, the molecular mechanism underlying 6-OHDA-induced insults in

Correspondence: Yoshiro Saito, Doshisha University, 1-3 Miyakodani, Tatara, Kyotanabe, Kyoto 610-0394, Japan. Tel: +81-774-65-6258. Fax: +81-774-65-6019. Email: ysaito@mail.doshisha.ac.jp

ISSN 1071-5762 print/ISSN 1029-2470 online
DOI: 10.3109/10715760903536349

the brain, especially during the early events, has not been completely elucidated.

6-OHDA has been demonstrated to induce toxicity in a wide range of *in vitro* neuronal models, including the rat adrenal pheochromocytoma cell line, PC12 [5–7]. It has been reported that 6-OHDA is rapidly oxidized by molecular oxygen to yield superoxide anions, hydrogen peroxide, and 2-hydroxy-5-(2-aminoethyl)-1,4-benzoquinone (*p*-quinone) as follows [8]:

$$6\text{-OHDA} + O_2 \rightarrow p\text{-quinone} + H_2O_2 \quad \text{(reaction 1)}$$

It is thought that the reactive oxygen species (ROS) generated by 6-OHDA initiate cellular oxidative stresses. On the other hand, it has been reported that *p*-quinone mediates 6-OHDA-induced cell death [9]. It has been known that 6-OHDA is readily oxidized within a few minutes to produce H_2O_2 and *p*-quinone in the extracellular fluid rather than in intracellular fluid [7,8]. Since it has been shown that catalase, which is barely incorporated into cells, completely abolished the sole cytotoxic effects of H_2O_2, it is considered that the cytotoxicity of 6-OHDA in the presence of catalase might be primarily mediated by *p*-quinone [7]. We have reported that H_2O_2 generated by 6-OHDA plays a pivotal role in the 6-OHDA-induced peroxiredoxin oxidation and cytochrome *c* release, while H_2O_2- and cytochrome *c*-independent caspase activation pathways are also involved in 6-OHDA-induced neurotoxicity [7]. It is believed that the latter cytotoxic activity, which is estimated from the cytotoxicity of 6-OHDA in the presence of catalase, is mediated by *p*-quinone. Quinones are biologically active compounds and all quinones are redox cycling agents that generate ROS. In contrast, partially substituted quinones including *p*-quinone can function as arylating agents that react with cellular nucleophiles such as thiols, thereby forming covalently linked quinone-thiol Michael adducts [10]. Differences in the endoplasmic reticulum (ER) stress induction property of arylating and non-arylating quinones have been reported [11]. It has been shown that glutathione (GSH) is capable of reacting with *p*-quinone at the second-position to form 2-S-(glutathionyl)-6-OHDA [12]. Furthermore, it has been reported that the GSH and N-acetyl cysteine (NAC) effectively attenuate the 6-OHDA-induced cytotoxicity in cultured cells [7,13]. Although there is a difference in the O_2 concentration between *in vitro* and *in vivo* conditions, a few studies have reported the protective effects of thiol compounds against 6-OHDA neurotoxicity *in vivo*; for example, Soto-Otero et al. [14] have reported that thiol compounds such as GSH and NAC can prevent the loss of tyrosine hydroxylase induced by 6-OHDA *in vivo*, as revealed by immunostaining [14]. However, the molecular mechanism underlying 6-OHDA-induced neurotoxicity *in vivo* has not been completely elucidated.

In the present study, we analysed the proteomes of the striatum and midbrain of a 6-OHDA-treated neonatal rat—an ADHD model—and compared the alterations in the *in vivo* experiment with those in the *in vitro* experiment. Among the omic technologies, proteomics is a rapidly developing analytical field of study and is becoming a significant source of information for protein expression and post-translational modification. The information regarding protein expression and protein modification is important to understand the cellular stress response. We found that the expression of 58-kDa glucose-regulated protein 58 (Grp58) and C/EBP homologous protein (CHOP) was altered in both *in vivo* and *in vitro* situations, suggesting that ER stress via the formation of H_2O_2 and *p*-quinone is involved in the insults induced by 6-OHDA *in vivo*.

Materials and methods

Materials

6-OHDA (purity, more than 97%) and desipramine were purchased from Sigma-Aldrich (St. Louis, MO). GSH and 3-(4,5-dimethylthiazol-2-yl)-2,5-diphenyl tetrazolium bromide (MTT) were purchased from Nacalai Tesque (Kyoto, Japan). CyDye difference gel electrophoresis (DIGE) Fluor Cy2, Cy3 and Cy5 dyes were purchased from GE Healthcare Bioscience (Uppsala, Sweden). Lambda protein phosphatase (λ-PPase) was purchased from BioLabs Inc. Hydrogen fluoride (HF)-pyridine was obtained from Fluorochem Ltd. (Derbyshire, UK).

Animals

All the experiments were conducted in accordance with the Guidelines for the Care and Use of Laboratory Animals of the National Institute of Advanced Industrial Science and Technology, Japan. Pregnant female Wistar rats were purchased from Clea Japan (Tokyo, Japan) 2 weeks after insemination. The animals were individually housed in acrylic cages illuminated under a 12-h light/dark cycle (light: 07:00–19:00) at 22°C and were provided tap water and laboratory chow (Oriental Yeast, Tokyo, Japan).

Treatments of rats with 6-OHDA and dissection of the brain

Male rat pups (5-days-old) weighing ~ 10 g were intraperitoneally administrated 25 mg/kg of desipramine, as described previously [2]. After 30 min, 100 μg of 6-OHDA dissolved in 0.9 % NaCl was administered intracisternally. Control pups received an intracisternal injection of vehicle under similar conditions. Pups were randomly assigned to lactating

dams (5–7 pups/dam) and were weaned at 3 weeks of age. Rats were decapitated at 6 h, 12 h, and 1–3 weeks after treatment with 6-OHDA. The whole brain was removed rapidly and placed on an ice-cold glass plate with the ventral surface facing upward. The striatum and midbrain were separated from the whole brain. Tissue samples were frozen in liquid nitrogen and stored at −80°C.

Protein assay

Protein concentration was determined by using the bicinchoninic acid (BCA) protein assay kit (Pierce Biotechnology, Inc., Rockford, IL) with bovine serum albumin as a standard.

Determination of catecholamine contents

Catecholamine levels were measured in the striatum of rats after 6-OHDA treatment as described previously [3]. Tissue samples were homogenized in 0.5 ml of 0.2 M perchloric acid containing 100 μM ethylenediaminetetraacetate (EDTA)-2Na and 100 ng of isoproterenol (internal standard). After centrifugation at 20 000 × g for 15 min, the supernatant was transferred to another tube and the pH was adjusted to 3 by adding 1 M sodium acetate. The samples were subjected to high-performance liquid chromatography (HPLC). The catecholamines were separated using a reverse-phase column (4.6 × 150 mm) Eicompak MA-5ODS (Eicom, Kyoto, Japan) maintained at 25°C. A 0.83 M citrate-sodium acetic acid buffer, pH 3.5, containing 230 mg/L octane-sulphonic acid, 5 mg/L EDTA-2Na and 17% methanol was used as the mobile phase and the flow rate was adjusted to 1.0 mL/min. Dopamine (DA) and norepinephrine (NE) were detected by an electrochemical detector (ECD-100; Eicom) at +750 mV using Ag/AgCl surface electrodes. DA (SIGMA H8502) and NE (SIGMA A7275) were used as a standard. The results were shown as nanograms per milligram of protein.

2D-DIGE and image analysis

The striatum and midbrain samples were lysed by sonication in an appropriate lysis buffer for 2D-DIGE analysis [8 M Urea, 30 mM Tris-HCl, and 4% 3-[(3-chol-amidopropyl)-dimethylammonio]-1-propane sulphonate (CHAPS), pH 8.5]. Protein extracts were labelled according to the manufacturer's instructions (CyDye DIGE fluor minimal labelling kit; GE Healthcare). Protein extracts (25 mg each of control or 6-OHDA-treated samples) were labelled with 200 pmol of Cy3 or Cy5 fluorescent dye on ice for 30 min in the dark. Equal amounts of proteins from four samples were combined to generate an internal pool. This pool was labelled with Cy2 fluorescent dye and included in all the gels run. The labelling reaction was quenched with 10 mM lysine. After the labelling reaction, three samples, along with a pool aliquot, were mixed and run on a single gel. The samples were mixed with 2D-DIGE sample buffer [8 M Urea, 4% CHAPS, 130 mM dithiothreitol (DTT), and 0.5% immobilized pH gradient (IPG) buffer, pH 4–7]. The strips were rehydrated with Cy-labelled samples in the dark overnight. The first-dimensional isoelectric focusing (IEF) was performed using the IPGphor apparatus (GE Healthcare) as recommended by the supplier. The IPG strip was equilibrated for 15 min with gentle shaking in 100 mM Tris-HCl, pH 8.8, containing 6 M Urea, 2% (w/v) sodium dodecyl sulphate (SDS), 65 mM DTT, 30% glycerol, and trace of bromophenol blue. Iodoacetamide (53 mM) was added to the second equilibration buffer instead of DTT, and the strips were incubated for 15 min in this solution. The second-dimensional separation was achieved by performing 12.5% SDS-polyacrylamide gel electrophoresis (SDS-PAGE). Proteins were visualized by using fluorescence scanner at appropriate wavelengths for Cy2, Cy3, and Cy5 dyes (Typhoon 9400; GE Healthcare). Image analysis was performed using the DeCyder 5.0 software (GE Healthcare). The differential in-gel analysis (DIA) module was used for pairwise comparisons of each control and 6-OHDA treatment samples and calculation of normalized spot volumes/protein abundances. The spot maps corresponding to the four gels were used to calculate the average abundance changes and paired Student's *t*-test derived *p*-values for each protein across the four gels. This was achieved by using the DeCyder biological variation analysis (BVA) module and the Cy3/Cy2 and the Cy5/Cy2 ratios for each protein.

In-gel trypsin digestion and identification by liquid chromatography/mass spectrometry (LC/ MS)

Differentially expressed protein spots were excised from a 2-D gel stained with SYPRO Ruby dye, transferred to sterile 1.5 mL micro-centrifuge tubes, and digested with sequencing-grade modified trypsin according to a previously described procedure with minor modifications [15]. Briefly, protein spots were washed twice with 100 mM ammonium bicarbonate (pH 8.5) and then dehydrated with acetonitrile. The gel pieces were reduced with 10 mM DTT at 56°C for 45 min and alkylated with 50 mM iodoacetamide for 45 min at room temperature in the dark in ammonium bicarbonate buffer. The gel pieces were washed with ammonium bicarbonate buffer, dehydrated with acetonitrile, and dried. They were subjected to in-gel trypsin digestion with 20 μL of 20 mM ammonium bicarbonate buffer containing 15 ng/μL trypsin at 37°C for 18 h. The peptides were extracted from the

gel pieces twice with 20 μL of 20 mM ammonium bicarbonate buffer and thrice with 20 μL of 0.5% trifluoroacetic acid in 50% acetonitrile. The peptides yielded after the 5-step extraction procedure were pooled together and concentrated to 20 μL using a Speed Vac (Thermo Electron).

The peptide extracts were subjected to analyse using liquid chromatography–electrospray ionization–mass spectrometry (LC- ESI-MS/MS) which consisted of a low flow LC system with flow splitter (MAGIC 2002, Microm BioResoueces, CA) and an ion trap mass spectrometer (LCQ Deca, Thermo Fisher Scientific, MA, USA) interfaced with nanospray ion source (AMR Inc., Tokyo, Japan). The samples were injected to reverse-phase trap column (0.2 mm × 5 cm; MonoCap for fast-flow; GL Science, Tokyo, Japan). Concentrated and desalted sample by the trap column was eluted to a fast-equilibrating C18 capillary column (monolith-type column; i.d., 0.1 mm; length, 50 mm; GL Science) for the separation. The gradient profile consisted of a linear gradient from 5% of solvent B [H_2O/acetonitrile/formic acid, 10/90/0.1 (v/v/v)] to solvent A [H_2O/acetonitrile/formic acid, 98/2/0.1 (v/v/v)] for a duration of 40 min at a flow rate of 300 nL/min. The separated sample was analysed in the data-dependent positive acquisition mode on an ion trap mass spectrometer via fused-silica Fortis Tip emitter (o.d., 150 μm; i.d., 20 μm; AMR, Inc). The following dynamic exclusion settings were used: repeat count of 2, repeat duration of 0.5 min, exclusion list size of 25, and exclusion duration of 3.0 min. After obtaining each scan (m/z 400–2000), a data-dependent triggered MS/MS scan was acquired for the most intense parent ion.

Database search and protein identification

Acquired LC-MS/MS data were transferred to a local MASCOT (version 2.1, Matrix Science, Inc., London, UK) server (www.matrixscience.com) for querying all MS/MS ion searches against National Center for Biotechnology Information (NCBInr, Rat Protein Database, updated on 9 September 2006). The typical parameters used in the MASCOT MS/MS ion search were as follows: maximum of one trypsin miss cleavage; fixed modification, cysteine carbamidomethylation; variable modification, methionine oxidation; peptide mass tolerance, ± 2 Da threshold ($p < 0.05$); minimum ion counts, 0; and fragment mass tolerance, ± 0.8 Da.

1D-PAGE and 2D-PAGE for western blotting

For 1D-PAGE, an equal amount of protein from each sample (30 μg) was electrophoresed on 12.5% SDS-PAGE. For the first dimension of 2D-PAGE, IPG gel strips (pH 4–7; non-linear, 7 and 13 cm) were used. The samples were mixed with rehydration buffer [9 M Urea, 5% CHAPS, 65 mM dithioerythreitol (DTE), 0.5% ampholyte (pH 4–7)] and applied on a gel (75 μg protein for a 7-cm gel and 150 μg for a 13-cm gel). The voltage for the electrophoresis was increased stepwise to 5000 V or 8000 V at maximum current of 200 mA for 3–5 h.

After the samples were separated by either 1D-PAGE or 2D-PAGE, they were transferred onto polyvinylidene fluoride (PVDF) membranes (Millipore, Bedford, MA). The membranes were blocked in Tris-buffered saline (pH 7.4) containing 0.1% Tween 20 (TBS-T) by a semi-dray electroblotter (Bio-Rad, CA), incubated with rabbit anti-Grp58 polyclonal antibodies (StressGen Biotechnologies) for 3 h, washed with TBS-T, incubated with horseradish peroxidase-conjugated secondary antibodies against rabbit IgG at least for 1 h and washed with TBS-T. Immunoreactivity to the anti-Grp58 antibodies was visualized using an enhanced chemiluminescence system (Millipore Co.).

Protein phosphatase treatment

The samples were incubated with 100 unit of λ-PPase in λ-PPase buffer (50 mM Tris-HCl, 0.1 mM Na_2EDTA, 5 mM DTT, 0.01% Triton X-100, pH 7.5) for 3 h at 30°C. Next, the samples were separated with 2D-PAGE and immunoblotted using anti-Grp58 antibodies.

Dephosphorylation of proteins using HF-pyridine

Dephosphorylation of proteins using HF-pyridine was performed as described previously [16]. Samples were dephosphorylated using HF-pyidine, neutralized with NaOH, mixed with chloroform/methanol (4:1), and the protein layer was subjected to 2D-PAGE and immunoblotted using anti-Grp58 antibodies.

Undifferentiated PC12 cell cultures

The rat pheochromocytoma cell line PC12 was routinely maintained in Dulbecco's modified Eagle's medium (DEM/F-12) containing 10% heat-inactivated foetal bovine serum and 5% heat-inactivated horse serum at 37°C under an atmosphere of 95% air and 5% CO_2. In order to analyse the toxicity of 6-OHDA, the PC12 cells were grown on plates at a density of 2×10^5 cells/mL. After the cells adhered to the plates (16–18 h), they were treated with 6-OHDA at different concentrations for the indicated times. For determining the cell viability, MTT assay was performed for the indicated periods. The cells were incubated with 0.5 mg/mL MTT in fresh

medium at 37°C for 2 h. Isopropyl alcohol containing 0.04 N HCl was added to the culture medium (3:2 by volume) and mixed through by a pipette until the formazan dissolved completely. The optical density of formazan was measured at 570 nm using a Multiskan Ascent plate reader (Theromo Labsystems, Helsinki, Finland).

Caspase activity assay

Caspase activity was measured by cleavage of the Asp-Glu-Val-Asp (DEVD) peptide-conjugated 4-methyl-coumaryl-7-amide (AMC), the Ile-Glu-Tyr-Asp (IETD)-AMC, and the Leu-Glu-His-Asp (LEHD)-AMC, according to the protocol outlined by the manufacturer of APOPCYTO Caspase Fluorometric Assay kit (Medical & Biological Laboratories). Substrate cleavage, which resulted in the release of AMC (excitation and emission wavelengths of 380 nm and 460 nm, respectively), was measured by using a Multiskan Ascent plate reader (Thermo Labsystems). Absorbance units were converted to pmoles of AMC using a standard curve generated by free AMC.

Statistical analysis

Data have been expressed as mean ± SD of at least three separate experiments. Statistical analysis was performed by the analysis of variance (ANOVA) using Dunnett's and Tukey's tests for multiple comparisons. The analysis method has been described in each figure legend.

Results

Toxic insults on dopaminergic neurons of neonatal rats treated with 6-OHDA

We have previously reported that the spontaneous motor activity of 5-day-old neonatal rats treated with both 6-OHDA is significantly increased at 4–5 weeks of age [2]. In order to elucidate the toxic insults on dopaminergic neurons, especially during the early phases, induced by 6-OHDA, the DA and NE contents in the striatum were measured at each sampling time after 6-OHDA administration. DA content significantly decreased at 12 h, but not at 6 h, after 6-OHDA treatment (Table I). The DA content continued to decrease up to 3 weeks after 6-OHDA treatment; it was 254.6 ± 28.6 ng/mg protein and 20.8 ± 18.8 ng/mg protein in the control and 6-OHDA-treated rats, respectively. There was no significant difference in the NE content after 6-OHDA treatment. These results suggest that the insults of 6-OHDA on dopaminergic neurons along with neuronal loss occurred after 12 h of treatment.

Proteomic analysis of the striatum and midbrain in neonatal rats treated with 6-OHDA

In order to investigate the molecular mechanisms underlying dysfunction induced by 6-OHDA, protein extracts prepared from the striatum and midbrain of rats treated with 6-OHDA for 6 h to 3 weeks were labelled with fluorophore Cy2, Cy3, or Cy5 and analysed by Ettan DIGE system. Figures 1A and B show representative 2D-profiles of the samples from the control and 6-OHDA treated striatum. These images were analysed by using DeCyder software. On the basis of the differences in their normalized and averaged intensities on triplicate 2-D gels, we found that the density of four spots (numbers G1–G4) was significantly altered in the 6-OHDA-treated samples (Figures 1A and B). Those spots were identified as 58 kDa glucose-regulated protein (Grp58) by ESI-LC-MS/MS, which is also called protein disulphide isomerase A3 (PDI A3) and endoplasmic reticulum protein 57 (Erp57) [17]. Figures 1C and D show the time-dependent changes in the four spots derived from Grp58 in the striatum and midbrain of rats treated with 6-OHDA. After 6 h of 6-OHDA treatment, there was a significant increase in the density of spots G3 and G4, which returned to the basal levels within 12 h. This acidic shift of Grp58 suggests that it underwent post-translational modification. On the other hand, the density of spot G1 (Grp58) from the striatum and midbrain increased after 12 h, 1 week, and 2 weeks of 6-OHDA-treatment, indicating the induction of Grp58 protein. Collectively, these results suggest that Grp58 protein was temporarily altered and induced by 6-OHDA.

In order to investigate the post-translational modification of Grp58, we conducted western blot analysis. As shown in Figure 2A, the acidic spot shift of Grp58 was detected by western blot analysis. It has been reported that the acidic spot shift of Grp58 occurs due to its phosphorylation [18]. To determine whether Grp58 was phosphorylated by 6-OHDA-treatment, we treated the striatum sample with λ-PPase and subjected it to western blot analysis. Consequently, a slight decrease in the density of spot G3 and concomitant increase in the density of spot G1 were observed (Figure 2B). Furthermore, the HF-pyridine treatment effectively reduced the acidic spot shift of Grp58 (Figure 2C). These results indicated that Grp58 is phosphorylated by 6-OHDA.

Induction of CHOP in the striatum and midbrain of rats treated with 6-OHDA

It has also been reported that 6-OHDA can induce ER stress and CHOP expression via pancreatic ER kinase (PERK) signalling pathway [19]. Furthermore, Grp58 is a stress protein that is localized in the lumen of ER whose expression is induced in several stress

Table I. Effects of neonatal treatment with 6-OHDA on endogeneous catecholamine levels in the rat striatum.[a]

	0 h	6 h	12 h	24 h
DA level				
Control	199.0 ± 9.4	220.4 ± 7.4	227.9 ± 19.7	225.5 ± 7.6
6-OHDA	234.3 ± 14.2	246.4 ± 8.5	45.5 ± 6.0*	63.4 ± 27.8*
NE level				
Control	18.4 ± 0.9	16.1 ± 1.8	20.2 ± 1.5	17.5 ± 14.0
6-OHDA	17.3 ± 1.0	19.4 ± 4.3	16.6 ± 1.7	14.0 ± 3.8

[a]Rats received intracisternal administration of 6-OHDA after intraperitoneal injection of desipramine at 5 days of age. At each time, rats were sacrificed and catecholamine levels were measured by HPLC-ECD as described in Materials and methods. Results are expressed as ng/mg protein and mean ± SD.
*$p < 0.05$ vs respective control value (Student's *t*-test).

conditions [17,20]. On the basis of this background information, we attempted to determine the alterations in CHOP expression in the striatum and midbrain by 6-OHDA-treatment using western blot analysis. As shown in Figures 3A and B, CHOP protein level significantly increased by up to ~ 3-fold in the striatum and midbrain of rats treated with 6-OHDA for 6 h. These results indicate that not only Grp58 but also CHOP levels in the striatum and midbrain increased by 6-OHDA-treatment.

Cytotoxicity and caspase activation in the PC12 cells treated with 6-OHDA and the roles of hydrogen peroxide and p-quinone generated

In order to understand the molecular mechanism underlying the insults induced by 6-OHDA in the rat ADHD model, we next conducted *in vitro* experiments using PC12 cells. We previously reported that both H_2O_2 and *p*-quinone generated by 6-OHDA play unique roles in the 6-OHDA-induced cytotoxicity [7]. Since the cytotoxic effect induced by H_2O_2, which is the secondary product of 6-OHDA, was completely abolished in the presence of catalase, it was believed that 6-OHDA elicited its effect in the presence of catalase by means of *p*-quinone-mediated cytotoxicity in PC12 cells. Cell viability assay based on the mitochondrial function suggested that 6-OHDA and H_2O_2 exhibit similar levels of cytotoxicity [7], while the *p*-quinone-induced mitochondrial toxicity is lower than that induced by 6-OHDA (Figure 4A).

Furthermore, we assessed the activity of caspases, which are required for the execution of the intrinsic apoptosis pathway. In this experiment, we used 100 μM of 6-OHDA, which is the cytotoxic concentration generating 50 μM of H_2O_2 and 100 μM of *p*-quinone [7]. Concomitant with the results of our previous study, the caspase 3 enzyme activity in 6-OHDA- and *p*-quinone-treated cells was higher than that of the H_2O_2-treated cells (Figure 4B). Interestingly, it was observed that both caspase 8 and caspase 9 were activated under each stress condition (Figure 4B). Taken together, these results suggest that H_2O_2 and *p*-quinone generated from 6-OHDA play unique roles in the 6-OHDA-induced cytotoxicity: *p*-quinone possesses potent biological activity to activate caspases.

Induction of Grp58 and CHOP in PC12 cells treated with 6-OHDA and the roles of hydrogen peroxide and p-quinone generated

In order to understand the roles of reactive species responsible for the alteration observed in the *in vivo* proteomic analysis, we analysed the post-translational modification and protein induction in 6-OHDA-treated PC12 cells. Although reproducible results were not obtained for the phosphorylation of Grp58 (data not shown), significant induction of Grp58 and CHOP proteins was observed at cytotoxic concentration of 6-OHDA applied for 24 h (Figure 5A). Time-dependent analysis revealed that these proteins were induced after 6 h of treatment with 6-OHDA (Figures 5B and C). In order to understand the role of reactive species generated by 6-OHDA, we analysed the effect of H_2O_2 and *p*-quinone. As shown in Figure 5D, both H_2O_2 and *p*-quinone increased Grp58 and CHOP levels. It has been known that GSH can protect the insults induced by 6-OHDA via the suppression of reaction 1 as well as the elimination of generated reactive species [6,7,14]. At an effective concentration against cell death induced by 6-OHDA [7], GSH significantly attenuated the increase of Grp58 and CHOP levels (Figure 5D).

In order to determine whether the observations described above apply to other arylating quinones or are specific to *p*-quinone, we analysed the effect of the arylating 1,4-benzoquinone. As shown in Figures 5E and F, 1,4-benzoquinone increased the levels of both Grp58 and CHOP, suggesting that arylating quinone can induce both proteins. It was further confirmed that ER stress inducer tunicamycin could increase Grp58 and CHOP levels (Figures 5E and F). These evidences suggest that H_2O_2 and *p*-quinone play a significant role in the induction of Grp58 and CHOP proteins via ER stress response.

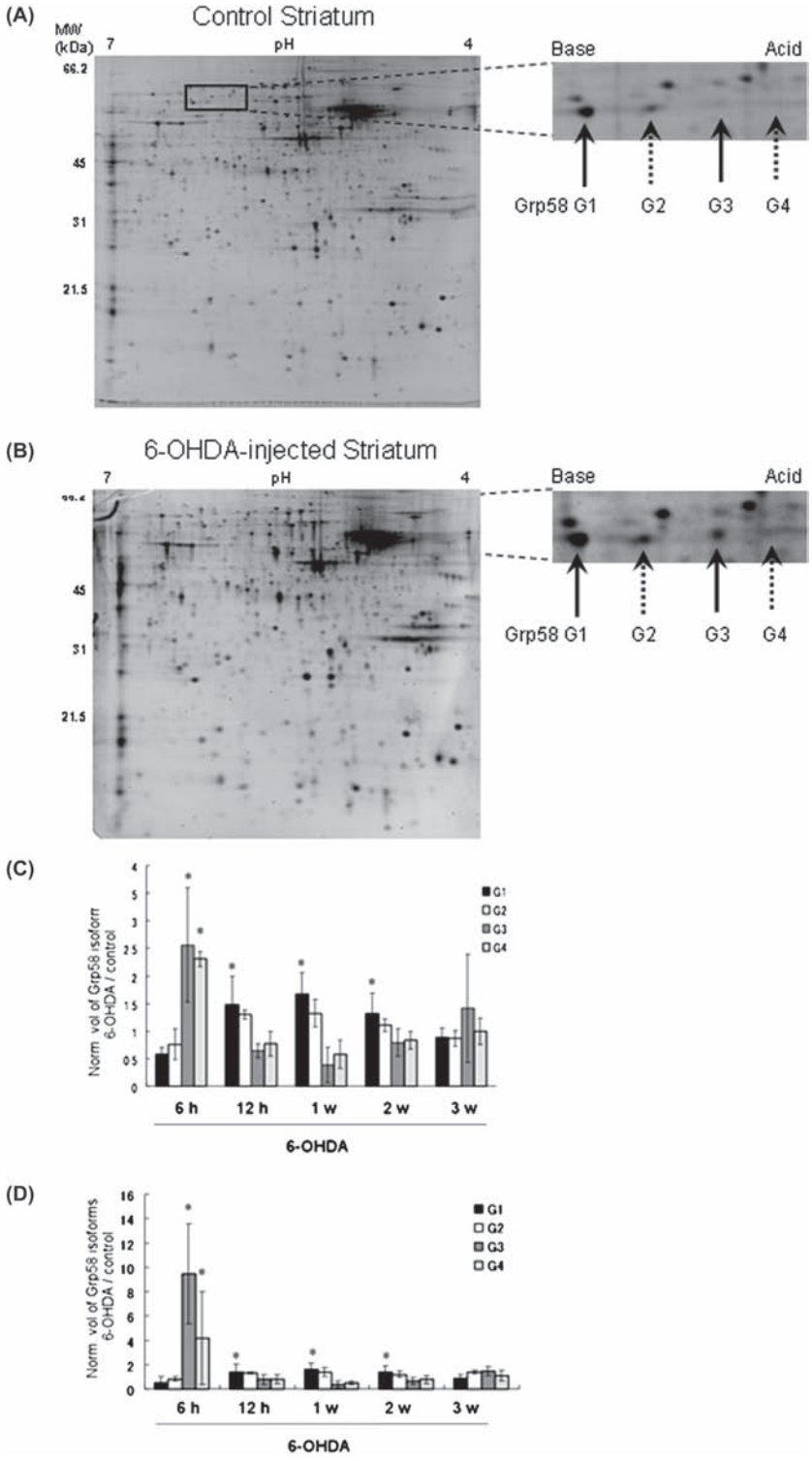

Figure 1. Proteomic analysis of the striatum and midbrain in neonatal rats treated with 6-OHDA. Representative 2D-gel image of the striatum of rats treated with control saline (A) and 6-OHDA (B) using pre-cast IPG strip (13 cm, pH 4–7) in the first dimension; 75 μg of protein was loaded. The protein spots marked by arrow indicate Grp58 identified by using LC/MS analysis. Time-dependent changes in the four spots derived Grp58 in the striatum (C) and midbrain (D) of rats treated with 6-OHDA. The results were expressed as relative spot normalize volumes compared to control and reported as mean ± SD ($n = 4$). $*p < 0.01$ in comparison with the control sample on each time (*t*-test).

Discussion

6-OHDA has been widely used as a neurotoxin for generating not only PD models but also ADHD models; however, the molecular mechanism underlying 6-OHDA-induced neurotoxicity *in vivo*, especially during the early events, has not been completely elucidated. In the present study, we demonstrated that in an ADHD model, 6-OHDA induces Grp58

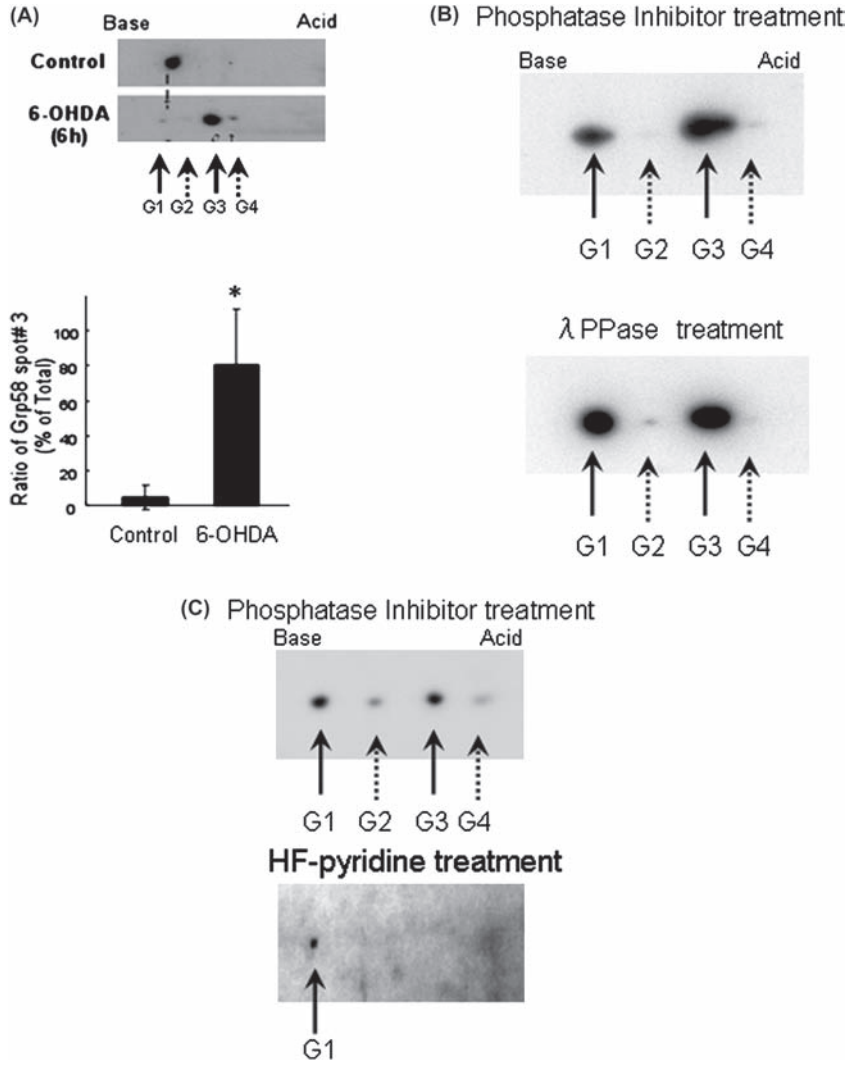

Figure 2. Phosphorylation of Grp58 in the striatum of rats treated with 6-OHDA. (A) Western blot analysis of the striatum of rats treated with 6-OHDA for 6 h using an anti-Grp58. The relative spot densities of spot G3 calculated using Phoretix 2D software are shown. $*p < 0.01$ in comparison with the control sample (*t*-test). (B) The effect of phosphatase treatment. The striatum samples treated with phosphatase in the presence or absence of phosphatase inhibitor were subjected to western blot analysis. (C) Effect of dephodphorylation using HF-pyridine. The striatum samples treated with HF-pyridine were subjected to western blot analysis.

phosphorylation and CHOP elevation at 6 h and then induces Grp58 elevation and DA depletion at 12 h after treatment. On the basis of the *in vitro* experimental results using PC12 cells, it is considered that H_2O_2 and *p*-quinone generated by 6-OHDA play a significant role in the induction of Grp58 and CHOP. Collectively, it is considered that the conversion of 6-OHDA to H_2O_2 and *p*-quinone might occur in the rat brain, and ER stress induced by these compounds might be responsible for the neurotoxicity of 6-OHDA.

Grp58 is a member of the protein disulphide isomerase family and catalyses disulphide bond formation in glycoprotein and is also induced under cellular stress conditions [17]. It has also been reported that Grp58 phosphorylation is induced by a variety of stimuli such as leptin in the liver [18], angiotensin II in the smooth muscle cells [21], and gamma-knife surgery in the brain [22]. Grp58 is a molecular chaperon localized in the lumen of the ER; it possesses an ER-retention signal in the C-terminal region. It is thought that the sub-cellular localization of Grp58 is regulated by the phosphorylation of the tyrosine and serine residues [23]. Previous data revealed the association between Grp58 and signal transducer and activator of transduction 3 (STAT3), and it has been postulated that the phosphorylation of Grp58 might release STAT3 from the plasma membrane compartment, resulting in the activation of the down-stream signal transduction pathway [24,25]. STAT3 is a signalling molecule that mediates the activation of several cytokines and growth factors. In the present study, we could detect the increase in Grp58 phosphorylation in the *in vivo* experiments, but not in the *in vitro* experiments performed using PC12 cells. At present, it is not clear why Grp58 phosphorylation is

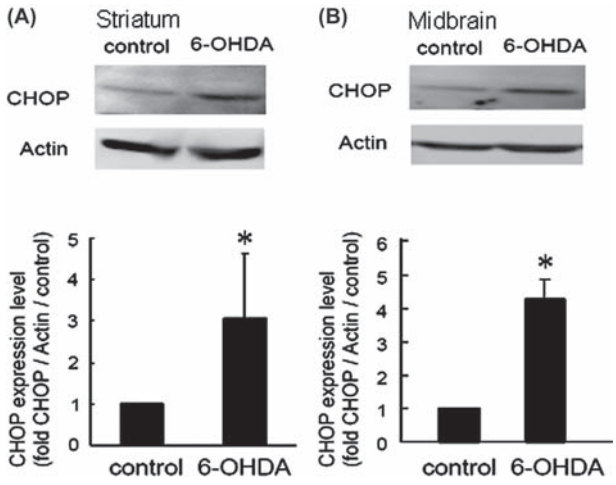

Figure 3. Induction of CHOP in the striatum and midbrain of rats treated with 6-OHDA. Western blot analysis of the striatum (A) and midbrain (B) of rats treated with 6-OHDA for 6 h were conducted by using anti-CHOP polyclonal antibodies. The relative densities calculated using Phoretix 2D software are shown. $*p < 0.01$ in comparison with the control sample (*t*-test).

induced by 6-OHDA *in vivo*, but not in vitro. Since it is considered that Grp58 phosphorylation-inducing stimuli such as angiotensin II and gamma-knife survey induce oxidative stress, it has been postulated that reactive species generated by 6-OHDA are responsible for the phosphorylation of Grp58 *in vivo*; however, the detailed molecular mechanism has not yet been elucidated. In order to understand the biological significance of Grp58 phosphorylation, it is necessary to identify the kinase responsible for Grp58 phosphorylation and the mechanism associated with the activation of this kinase.

As mentioned above, it has been reported that Grp58 expression is induced under a variety of cellular stress conditions such as glucose starvation [20], viral infection [26], and dopamine [27]. These conditions might result in the misfolding of proteins within the ER and the induction of the transcription factors such as activating transmembrane precursors 4 (ATF4) and CHOP-mediators of ER stress response. Gene chip analysis in the dopaminergic cell line MN9D treated with 6-OHDA has revealed that Grp58 and CHOP transcripts are increased by 6-OHDA [19]. It has been known that not only oxidative stress induced by H_2O_2 but also the electrophilic quinone, namely arylating quinone, can induce ER stress response [11]. The electrophilic quinone can function as an arylating agent that can react with nucleophiles such as the reduced sulphydryl groups in glutathione and cysteine or the cysteinyl residues in the proteins to form covalently-linked quinone-thiol adducts [10]. We previously reported that the arylating quinone, γ-tocopheryl quinone, but not the non-arylated α-tocopheryl quinone, can induce ER stress and adaptive response involving CHOP and ATF4 induction [28]. The ER, where the oxidative

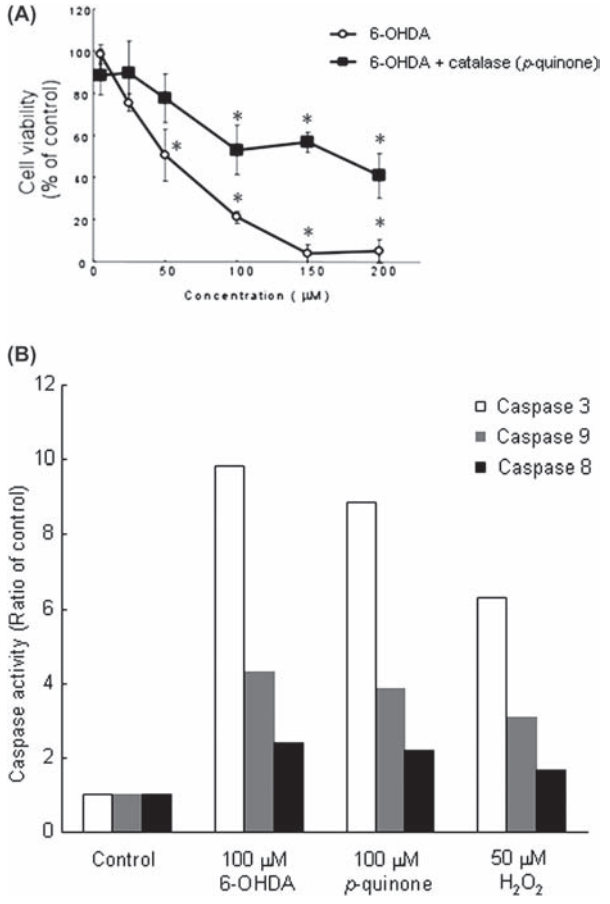

Figure 4. Effect of 6-OHDA and *p*-quinone on the viability and caspase activity of PC12 cells. (A) The cells were treated with variable amounts of 6-OHDA (open circle) in the presence (*p*-quinone, closed square) or absence (open circle) of 50 U/ml calatase for 24 h, and the viability was measured by MTT assay, as described in Materials and methods. $*p < 0.05$ when compared with control (Dunnett, ANOVA). (B) The cells were exposed to 100 μM 6-OHDA, 100 μM *p*-quinone or 50 μM H_2O_2 for 12 h, and were subjected to the enzyme assay using DEVD-AMC (Caspase 3 like), LEHD-AMC (caspase 9 like), and IEHD-AMC (caspase 8 like) as a substrate, as described under Materials and methods. The values represent the means for duplicate.

protein folding leads to the formation of disulphide bonds, is one of the most susceptible organelles to oxidation [29]. The relative abundance of oxidized glutathione (GSSG) compared with the reduced form of glutathione in the ER lumen has led to the assumption that GSSG serves as the oxidizing equivalent during protein folding [30]. Therefore, the ER is vulnerable to oxidative stress. Exogenously added H_2O_2 is known to diffuse rapidly into cells and react with cellular components and antioxidants [31], while arylating *p*-quinone might attack the nucleophiles in the cells. It has been observed that H_2O_2 plays an important role in the mitochondrial insults induced by 6-OHDA, while the knowledge on the effect of *p*-quinone is limited [7]. In view of the insults against ER, the data shown in the present study suggest that both H_2O_2 and *p*-quinone generated by 6-OHDA can exhibit neurotoxicity by inducing ER stress.

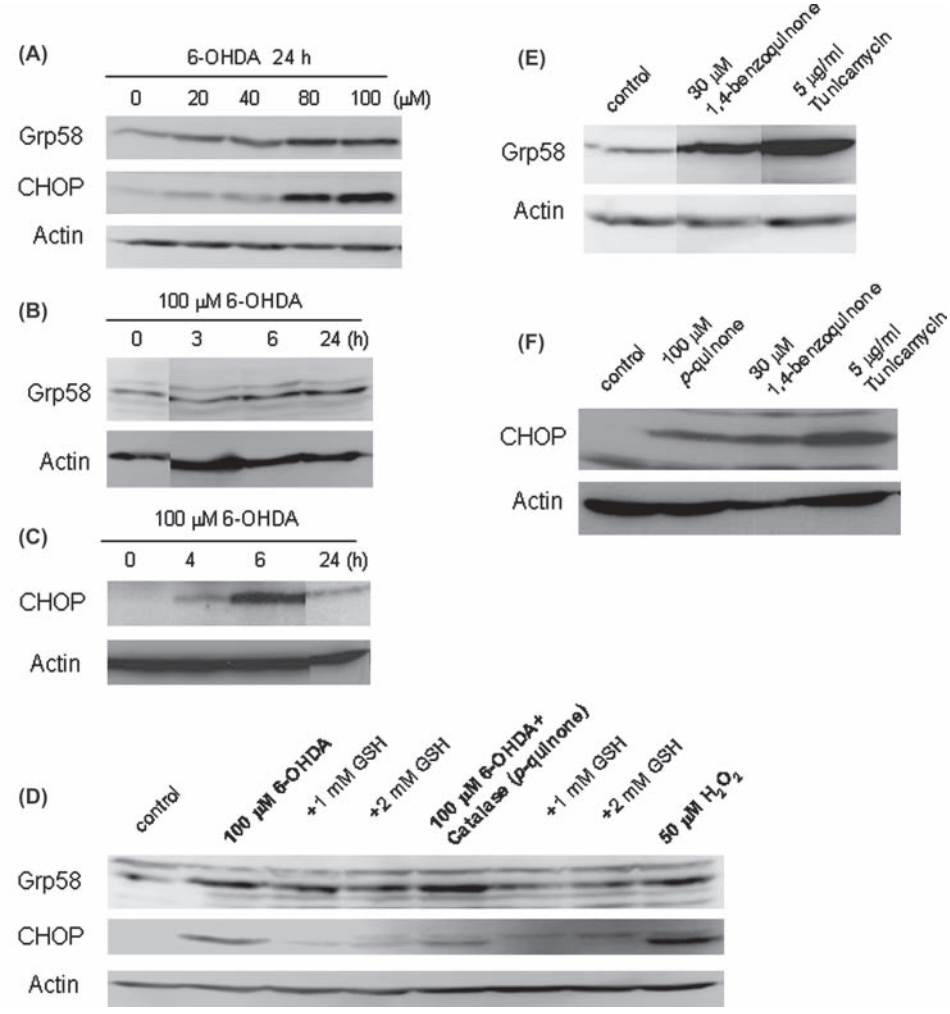

Figure 5. Effect of *p*-quinone and H_2O_2 on the Grp58 and CHOP levels in PC12 cells. (A) PC12 cells were treated with variable amounts of 6-OHDA for 24 h and subjected to western blot analysis using antibodies against Grp58 and CHOP. (B, C) The cell samples treated with 100 μM 6-OHDA for the indicated time periods were subjected to western blot analysis using antibodies against Grp58 (B) and CHOP (C). (D) The cell samples treated with 100 μM 6-OHDA, 100 μM *p*-quinone, or 50 μM H_2O_2 in the presence or absence of indicated amount of GSH for 6 h were subjected to western blot analysis using antibodies against Grp58 and CHOP. (E, F) The cell samples treated with 30 μM 1, 4-benzoquinone or 5 μg/ml tunicamycin for 6 h were subjected to western blot analysis using antibodies against Grp58 (E) and CHOP (F).

It has been reported that 6-OHDA treatment causes loss of GSH *in vivo* and *in vitro* [32,33]. On the other hand, it has been reported that GSH can suppress the neurotoxicity of 6-OHDA *in vivo* and *in vitro* [6,14]. We previously reported the significant protective effects of thiol compounds such as GSH and NAC against 6-OHDA-induced cell death in PC12 cells [7]. It has been reported that thiol compounds can suppress the conversion of 6-OHDA to H_2O_2 and *p*-quinone by acting against transition metals [14]. It is also known that GSH can accelerate the reduction of H_2O_2 to water in combination with glutathione peroxidase [34]. Furthermore, it has been demonstrated that GSH directly diminishes the electrophilic properties of arylating *p*-quinone [12]. Collectively, it is postulated that thiol compounds like GSH exhibit neuroprotective effects against 6-OHDA by not only suppressing the conversion of 6-OHDA but also eliminating the generated reactive species. In fact, we observed that GSH elicited a protective effect against the 6-OHDA-induced elevation of Grp58 and CHOP (Figure 5D), suggesting that GSH can inhibit ER stress induced by 6-OHDA. NAC is readily taken up by cells and subsequently acts as the source of cellular GSH, while it is known that GSH is barely incorporated into cells. Therefore, it is considered that GSH exhibits the inhibitory effect against the 6-OHDA-induced elevation of Grp58 and CHOP in the extracellular fluid. The cytoprotective effects of GSH also suggest that the conversion of 6-OHDA to H_2O_2 and *p*-quinone in the extracellular fluid is a critical step in its cytotoxicity. Collectively, these observations emphasize the significance of developing neuroprotective therapy using thiol compounds

against neurodegenerative diseases involving the degradation of dopaminergic neurons.

In conclusion, the present study revealed that 6-OHDA induced the alteration of Grp58 and CHOP protein during the early phase in both *in vivo* and *in vitro* experiments and suggested that H_2O_2 and *p*-quinone generated by 6-OHDA elicit detrimental effects on dopaminergic neurons by inducing ER stress. Our results might contribute to the understanding of the molecular mechanism underlying the insults induced by 6-OHDA in ADHD and PD models.

Declaration of interest: The authors report no conflicts of interest. The authors alone are responsible for the content and writing of the paper.

References

[1] Blum D, Torch S, Lambeng N, Nissou M, Benabid AL, Sadoul R, Verna JM. Molecular pathways involved in the neurotoxicity of 6-OHDA, dopamine and MPTP: contribution to the apoptotic theory in Parkinson's disease. Prog Neurobiol 2001;65:135–172.

[2] Masuo Y, Ishido M, Morita M, Oka S. Effects of neonatal 6-hydroxydopamine lesion on the gene expression profile in young adult rats. Neurosci Lett 2002;335:124–128.

[3] Masuo Y, Ishido M, Morita M, Oka S. Effects of neonatal treatment with 6-hydroxydopamine and endocrine disruptors on motor activity and gene expression in rats. Neural Plast 2004;11:59–76.

[4] Masuo Y, Ishido M, Morita M, Oka S, Niki E. Motor activity and gene expression in rats with neonatal 6-hydroxydopamine lesions. J Neurochem 2004;91:9–19.

[5] Chen ZH, Yoshida Y, Saito Y, Sekine A, Noguchi N, Niki E. Induction of adaptive response and enhancement of PC12 cell tolerance by 7-hydroxycholesterol and 15-deoxy-delta(12,14)-prostaglandin J_2 through up-regulation of cellular glutathione via different mechanisms. J Biol Chem 2006;281:14440–14445.

[6] Hanrott K, Gudmunsen L, O'Neill MJ, Wonnacott S. 6-hydroxydopamine-induced apoptosis is mediated via extracellular auto-oxidation and caspase 3-dependent activation of protein kinase Cdelta. J Biol Chem 2006;281:5373–5382.

[7] Saito Y, Nishio K, Ogawa Y, Kinumi T, Yoshida Y, Masuo Y, Niki E. Molecular mechanisms of 6-hydroxydopamine-induced cytotoxicity in PC12 cells: involvement of hydrogen peroxide-dependent and -independent action. Free Radic Biol Med 2007;42:675–685.

[8] Cohen G, Heikkila RE. The generation of hydrogen peroxide, superoxide radical, and hydroxyl radical by 6-hydroxydopamine, dialuric acid, and related cytotoxic agents. J Biol Chem 1974;249:2447–2452.

[9] Izumi Y, Sawada H, Sakka N, Yamamoto N, Kume T, Katsuki H, Shimohama S, Akaike A. p-Quinone mediates 6-hydroxydopamine-induced dopaminergic neuronal death and ferrous iron accelerates the conversion of p-quinone into melanin extracellularly. J Neurosci Res 2005;79:849–860.

[10] Cornwell DG, Kim S, Mazzer PA, Jones KH, Hatcher PG. Electrophile tocopheryl quinones in apoptosis and mutagenesis: thermochemolysis of thiol adducts with proteins and in cells. Lipids 2003;38:973–979.

[11] Wang X, Thomas B, Sachdeva R, Arterburn L, Frye L, Hatcher PG, Cornwell DG, Ma J. Mechanism of arylating quinone toxicity involving Michael adduct formation and induction of endoplasmic reticulum stress. Proc Nat Acad Sci USA 2006;103:3604–3609.

[12] Liang YO, Plotsky PM, Adams RN. Isolation and identificaton of an *in vivo* reaction product of 6-hydroxydopamine. J Med Chem 1977;20:581–583.

[13] Shimizu E, Hashimoto K, Komatsu N, Iyo M. Roles of endogenous glutathione levels on 6-hydroxydopamine-induced apoptotic neuronal cell death in human neuroblastoma SK-N-SH cells. Neuropharmacology 2002;43:434–443.

[14] Soto-Otero R, Mendez-Alvarez E, Hermida-Ameijeiras A, Munoz-Patino AM, Labandeira-Garcia JL. Autoxidation and neurotoxicity of 6-hydroxydopamine in the presence of some antioxidants: potential implication in relation to the pathogenesis of Parkinson's disease. J Neurochem 2000;74:1605–1612.

[15] Kinumi T, Kimata J, Taira T, Ariga H, Niki E. Cysteine-106 of DJ-1 is the most sensitive cysteine residue to hydrogen peroxide-mediated oxidation *in vivo* in human umbilical vein endothelial cells. Biochem Biophys Res Comm 2004;317:722–728.

[16] Kuyama H, Toda C, Watanabe M, Tanaka K, Nishimura O. An efficient chemical method for dephosphorylation of phosphopeptides. Rapid Commun Mass Spectrom 2003;17:1493–1496.

[17] Ni M, Lee AS. ER chaperones in mammalian development and human diseases. FEBS Lett 2007;581:3641–3651.

[18] Kita K, Okumura N, Takao T, Watanabe M, Matsubara T, Nishimura O, Nagai K. Evidence for phosphorylation of rat liver glucose-regulated protein 58, GRP58/ERp57/ER-60, induced by fasting and leptin. FEBS Lett 2006;580:199–205.

[19] Holtz WA, O'Malley KL. Parkinsonian mimetics induce aspects of unfolded protein response in death of dopaminergic neurons. J Biol Chem 2003;278:19367–19377.

[20] Lee AS. Coordinated regulation of a set of genes by glucose and calcium ionophores in mammalian cells. Trends Biochem Sci 1987;12:20–23

[21] Tokutomi Y, Araki N, Kataoka K, Yamamoto E, Kim-Mitsuyama S. Oxidation of Prx2 and phosphorylation of GRP58 by angiotensin II in human coronary smooth muscle cells identified by 2D-DIGE analysis. Biochem Biophys Res Comm 2007;364:822–830.

[22] Hirano M, Rakwal R, Kouyama N, Katayama Y, Hayashi M, Shibato J, Ogawa Y, Yoshida Y, Iwahashi H, Masuo Y. Gel-based proteomics of unilateral irradiated striatum after gamma knife surgery. J Proteome Res 2007;6:2656–2668.

[23] Sehgal PB. Plasma membrane rafts and chaperones in cytokine/STAT signaling. Acta Biochim Polon 2003;50:583–594.

[24] Hirano N, Shibasaki F, Sakai R, Tanaka T, Nishida J, Yazaki Y, Takenawa T, Hirai H. Molecular cloning of the human glucose-regulated protein ERp57/GRP58, a thiol-dependent reductase. Identification of its secretory form and inducible expression by the oncogenic transformation. Eur J Biochem/FEBS 1995;234:336–342.

[25] Sehgal PB, Guo GG, Shah M, Kumar V, Patel K. Cytokine signaling: STATS in plasma membrane rafts. J Biol Chem 2002;277:12067–12074.

[26] Mazzarella RA, Marcus N, Haugejorden SM, Balcarek JM, Baldassare JJ, Roy B, Li LJ, Lee AS, Green M. Erp61 is GRP58, a stress-inducible luminal endoplasmic reticulum protein, but is devoid of phosphatidylinositide-specific phospholipase C activity. Arch Biochem Biophys 1994;308:454–460.

[27] Dukes AA, Van Laar VS, Cascio M, Hastings TG. Changes in endoplasmic reticulum stress proteins and aldolase A in cells exposed to dopamine. J Neurochem 2008;106:333–346.

[28] Ogawa Y, Saito Y, Nishio K, Yoshida Y, Ashida H, Niki E. Gamma-tocopheryl quinone, not alpha-tocopheryl quinone, induces adaptive response through up-regulation of cellular glutathione and cysteine availability via activation of ATF4. Free Radic Res 2008;42:674–687.

[29] van der Vlies D, Pap EH, Post JA, Celis JE, Wirtz KW. Endoplasmic reticulum resident proteins of normal human dermal fibroblasts are the major targets for oxidative stress induced by hydrogen peroxide. Biochem J 2002;366:825–830.
[30] Hwang C, Sinskey AJ, Lodish HF. Oxidized redox state of glutathione in the endoplasmic reticulum. Science 1992;257: 1496–1502.
[31] Antunes F, Cadenas E. Estimation of H_2O_2 gradients across biomembranes. FEBS Lett 2000;475:121–126.
[32] Garcia JC, Remires D, Leiva A, Gonzalez R. Depletion of brain glutathione potentiates the effect of 6-hydroxydopamine in a rat model of Parkinson's disease. J Mol Neurosci 2000; 14:147–153
[33] Lee CS, Park WJ, Ko HH, Han ES. Differential involvement of mitochondrial permeability transition in cytotoxicity of 1-methyl-4-phenylpyridium and 6-hydroxydopamine. Mol Cell Biochem 2006;289:193–200
[34] Takebe G, Yarimizu J, Saito Y, Hayashi T, Nakamura H, Yodoi J, Nagasawa S, Takahashi K. A comparative study on the hydroperoxide and thiol specificity of the glutathione peroxidase family and selenoprotein P. J Biol Chem 2002;277: 41254–41258.

This paper was first published Online on Early Online on 27 January 2010.